Transient and steady-state heat transfer for forced convection of helium gas in minichannels with various inner diameters

Xu, Feng
Liu, Qiusheng
Shibahara, Makoto

(Citation)
International Journal of Heat and Mass Transfer,191:122813

(Issue Date)
2022-08-01

(Resource Type)
journal article

(Version)
Accepted Manuscript

Transient and steady-state heat transfer for forced convection of helium gas in minichannels with various inner diameters

Feng Xu[1], Qiusheng Liu[*], Makoto Shibahara

Department of Marine Engineering, Graduate School of Maritime Sciences, Kobe University, 5-1-1, Fukaeminami-machi, Higashinada-ku, Kobe 658-0022, Japan

Abstract

An experimental research was carried out on steady-state and transient heat transfer characteristics for forced convection of helium gas in minichannels. Platinum minichannels with different inner diameters were heated by an exponential power source with a wide range of e-folding time of heat generation rate and cooled by forced convection of helium gas with different flow velocities, inlet temperatures, and inlet pressures. The diameter effect of minichannels on the transient and steady-state heat transfer was investigated. According to the results, the heat transfer coefficients were improved with a decrease in the inner diameters of minichannels under both transient and quasi-steady states. A significant enhancement was obtained by using a 0.8 mm diameter minichannel. For the steady-state heat transfer, a new correlation was acquired for the 0.8 mm diameter minichannel and the correlation of a 1.8 mm diameter minichannel was appropriate for a 2.8 mm diameter minichannel. The influence of Reynolds number on steady-state Nusselt number for the 0.8 mm diameter minichannel was more significant compared with the 2.8 and 1.8 mm diameter minichannels. The transient heat transfer correlations for the 0.8 and 2.8 mm diameter minichannels were obtained by introducing Fourier number, respectively.

Keywords: minichannel; diameter effect; transient heat transfer; forced convection; helium gas

---

[1] Present address of this author: Organization for Programs on Environmental Sciences, Graduate School of Arts and Sciences, The University of Tokyo, 3-8-1 Komaba, Meguro-ku, Tokyo 153-8902, Japan

[*] Corresponding author. E-mail: qsliu@maritime.kobe-u.ac.jp

Nomenclature

a	thermal diffusivity of helium gas, m^2/s
b	constant of Eq. (20)
A	inner surface area of experimental minichannel, m^2
c_h	specific heat of experimental minichannel, J/(kg·K)
$c_{p,g}$	specific heat of helium gas at constant pressure, J/(kg·K)
d	inner diameter of experimental minichannel, m
d_h	hydraulic diameter, m
Fo	$= a\tau/d^2$, Fourier number
h	heat transfer coefficient, $W/(m^2 \cdot K)$
h_{st}	steady-state heat transfer coefficient, $W/(m^2 \cdot K)$
I	direct current, A
L	total length of experimental minichannel, m
L_{ipt}	distance from entrance pressure transducer to entrance of experimental minichannel, m
L_{opt}	distance from exit pressure transducer to exit of experimental minichannel, m
L_e	effective length of experimental minichannel, m
Nu	$= hd/\lambda$, Nusselt number
Nu_{st}	$= h_{st}d/\lambda$, steady-state Nusselt number
Nu_{tr}	transient Nusselt number
P_{in}	inlet pressure, kPa
Pr	$= \nu/a$, Prandtl number
q	heat flux, W/m^2
Q	heat generation rate, W
$\dot{Q}$	heat generation rate per unit volume, W/m^3
Q_0	initial exponential heat generation rate per unit volume, W/m^3
r	radius of experimental minichannel, m
r_i	inner radius of experimental minichannel, m
r_o	outer radius of experimental minichannel, m
Re	$= ud/\nu$, Reynolds number
R_s	standard resistance, Ω

R_T	resistance of experimental minichannel, Ω
R_0	resistance of experimental minichannel at 0 ºC, Ω
t	time, s
T	temperature, K
T_a	average temperature of experimental minichannel, ºC
T_g	mean bulk temperature of helium gas, K
T_{in}	inlet temperature of helium gas, K
T_{out}	outlet temperature of helium gas, K
$T(r)$	temperature distribution of experimental minichannel, K
T_s	inner surface temperature of experimental minichannel, K
T_{so}	outer surface temperature of experimental minichannel, K
ΔT	temperature difference between T_s and T_g, K
u	flow velocity, m/s
V	volume of experimental minichannel, m^3
V_I	voltage difference through standard resistance, V
V_R	voltage difference through experimental minichannel, V
V_T	unbalanced voltage difference of double-bridge circuit, V
α	constant of Eq. (4)
β	constant of Eq. (4)
δ	thickness of experimental minichannel, m
λ	thermal conductivity, W/(m·K)
ν	kinematic viscosity, m^2/s
ρ_g	density of helium gas, kg/m^3
ρ_h	density of experimental minichannel, kg/m^3
τ	e-folding time of heat generation rate, s

1. Introduction

The global warming and energy shortage are the trend worldwide with the rapid advance of society and economy. The nuclear fusion can provide a safe, CO_2 emission-free, clean and virtually unlimited energy to achieve the sustainable development [1]. In the fusion reactor, around 80% of the fusion power generated from the tokamak is collected by the tritium breeding blanket [2]. The high heat derived from the plasma is taken away by the forced convection of coolant in pipes of the blanket [3]. The efficiency of fusion-to-thermal energy conversion can be increased by the heat transfer augmentation in the forced convection through channels. The mini/micro channel, classified with hydraulic diameters (d_h) by Kandlikar [4] as shown in **Table 1**, provides a large surface area for heat transfer within a given volume compared with a conventional channel. According to the literature [5-7], the forced convective heat transfer was enhanced in minichannels. The blanket using helium gas as a coolant and a carrier of energy is widely acceptable as a candidate blanket [8]. Therefore, the understanding of forced convective heat transfer for helium gas passing through minichannels is considered to contribute to the thermal design of the helium cooled blanket.

Table 1 The channel classification [4].

Conventional channels	$3\ \text{mm} < d_h$
Minichannels	$200\ \mu\text{m} < d_h \le 3\ \text{mm}$
Microchannels	$10\ \mu\text{m} < d_h \le 200\ \mu\text{m}$

A great number of studies on the steady-state heat transfer for forced convective flow in minichannels have been reported. Bucci et al. [9] used three stainless steel tubes with diameters of 0.172, 0.29, and 0.52 mm to experimentally investigate single-phase heat transfer and fluid flow of water through capillary tubes. With a decrease in the channel diameter, the experimental data were deviated more from classical correlations for heat transfer. Li et al. [10] developed two heat transfer correlations for FC-72 flowing through small tubes in turbulent region. The correlation for the 2.8 mm diameter tube was distinguished from that for 1 and 1.8 mm diameter tubes. Their work supported the channel classification suggested from Kandlikar [4]. Naphon and Khonseur [11] carried out a thermal-hydraulic experiment on forced convection of air in rectangular micro-channel heat sinks. They found that the pressure drop and heat transfer showed significant dependence on the micro-channel geometry configuration. Further, some heat transfer enhancement techniques were applied to the minichannels. Ho and Chen [12] experimentally investigated the heat transfer characteristics of Al_2O_3/water nanofluid in a rectangular minichannel heat sink with 1.2 mm hydraulic diameter. They found that the average heat transfer coefficients obtained by using the

Al_2O_3/water nanofluid were enhanced significantly compared with the pure water. Dixit and Ghosh [13] used straight, diamond, and offset minichannels to experimentally study the thermal-hydraulic characteristics for water in enhanced minichannel heat sinks at low Reynolds number. Compared with the diamond minichannels, a relatively higher Nusselt number was obtained by using the offset minichannels.

The plasma disruption is an off-normal event that causes severe damage to the in-vessel components and shortens the lifetime of the tokamak [14]. The sudden high-energy deposition on the plasma-facing components results in a transient high-thermal load [15]. Therefore, the knowledge of transient heat transfer for tube flow of helium gas is significant to the safety assessment of the helium cooled blanket. Compared with steady-state forced convective heat transfer, the investigations on transient state are relatively few. Abbrecht and Churchill [16] experimentally researched the fully developed turbulent tube flow of air in the thermal entrance region with a step increase in wall temperature. Soliman and Johnson [17] used an exponential heat source to experimentally and analytically investigate the transient mean wall temperature of forced convective flow over a flat plate. The measured heat transfer coefficient for water was lower than the analytical solution. Prajapati et al. [18] performed an experimental investigation on transient heat transfer performance for flow boiling and single-phase flow of water in uniform cross-section and segmented finned microchannels. The initial very high heat transfer coefficient had a sharp decline with time in the transient state and reached the constant value in the steady state. Recently, the experimental investigations on transient heat transfer for helium gas flowing over various heating elements with various shapes and sizes were carried out in our previous works [19-21]. The cylinders [19], flat plates [20], and twisted plates [21] were used as test heaters and the heat inputs raised exponentially. The geometric and dimensional effects of heaters on transient heat transfer were clarified and transient Nusselt number correlations for different heater configurations were obtained.

To the knowledge of the authors, there are few experimental studies on steady-state forced convective heat transfer of helium gas in minichannels. Especially, the experimental investigations on transient heat transfer for helium gas in minichannels heated with an exponentially increasing power are very rare. In the present research, an experimental investigation was carried out on both steady-state and transient heat transfer characteristics of helium gas flowing in different diameters minichannels using an exponentially increasing heat input. The diameter-effect of minichannels on transient and steady-state heat transfer was clarified by the comparison of measured heat transfer coefficients. The transient and steady-state heat transfer correlations were developed by dimensionless parameters.

2. Experimental apparatus and methods

2.1. Experimental loop and test section

The transient experimental system in the present research consisted of three parts: a heat input control system for exponential power escalations; a forced convection loop for helium gas; a data acquisition and processing system. Two surge tanks, a gas compressor, a vacuum pump, a flow meter, a cooler, pre-heaters, two filters and the core component test section constituted the test loop, which was reported in our previous works [22, 23]. The details of the experimental loop and test section are illustrated in **Fig. 1**. The high pure helium gas was employed as test fluid and the compressor was used for gas continuous circulation. The flow fluctuation was eliminated by the surge tanks during the compressor running. The regulation of gas temperature was carried out by the water-cooled cooler and pre-heaters made of heating wires. The flow meter was utilized to measure the flow velocity and the by-pass loop was used to change the flow velocity. At the compressor exit and flow meter entrance, the filters were installed to prevent any small particles from causing flow block. The gas temperature and pressure of the flow meter exit were measured by a K-type thermocouple and a pressure transducer.

The experimental minichannels used in the present research were three platinum tubes (d = 0.8, 1.8, 2.8 mm; δ= 0.1 mm; L = 100 mm) with a material purity of 99.99%. Before installation, the thermal stress in the platinum tube was eliminated by means of the anneal and the impurities on tube surface were removed by using an acetone solution. The 5 mm parts of both ends of the platinum tube were inserted and soldered to two copper plates. A variable power source provided a direct current to heat the platinum tube through the copper plates serving as electrodes. The effective length (L_e), which means the part heated by the direct current, of the three platinum tubes was around 90 mm. The entry length of each platinum tube was larger than 10 times of the inner diameter to keep the flow hydrodynamically fully developed in the turbulent regime [24]. For the thermal insulation from the surrounding environment, the platinum tube was installed in a small cylindrical space enclosed with two Bakelite blocks that also provided mechanical support. The platinum tube was thermally and electrically insulated from the rest of experimental apparatus by two Bakelite plates. The silicon sheets were used for seal in case of gas leakage. The K-type thermocouples and pressure transducers were installed in inlet and outlet of the test section for temperature and pressure measurement.

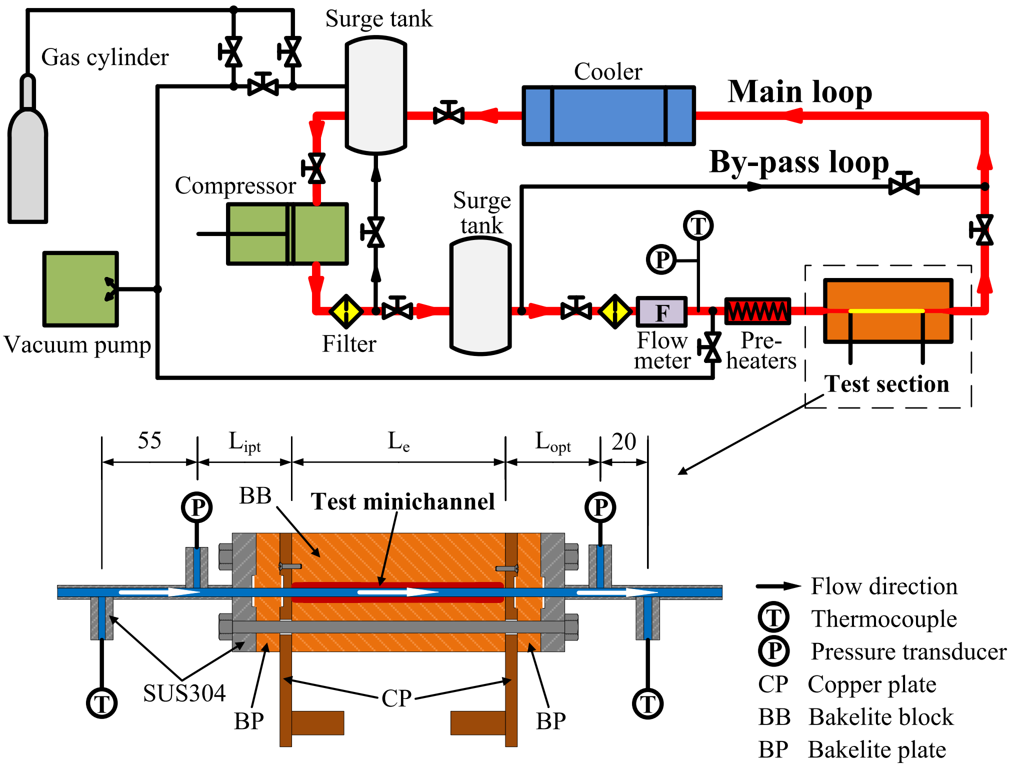

Fig. 1. The schematic diagram of the experimental loop and test section.

2.2. Data measurement method

The method for data measurement was reported in previous works [22, 23]. The experimental minichannel served as a branch of the double-bridge circuit for the data measurement with the method of resistance thermometry, as shown in **Fig. 2**. The electric equilibrium was obtained before the electrical heating process. When the experiment started, the temperature of the experimental minichannel increased due to the direct electric current ($I(t)$) passing through it. The heat generation rate of the experimental minichannel ($Q(t)$) was controlled and measured by the heat input system based on Joule heating:

$$Q(t) = V_R(t)I(t) \tag{1}$$

$$I(t) = V_I(t)/R_s \tag{2}$$

where $V_I(t)$ and $V_R(t)$ represent the voltage differences through the standard resistance (R_s) and the experimental minichannel, respectively. The electric resistance of the experimental minichannel ($R_T(t)$) increased with temperature causing the electric non-equilibrium, as calculated with the unbalanced voltage difference ($V_T(t)$):

$$R_T(t) = \frac{V_T(t)(R_2+R_3)}{I(t)R_2} + \frac{R_1R_3}{R_2} \tag{3}$$

The instantaneous voltage signals of the $V_I(t)$, $V_R(t)$, and $V_T(t)$ were simultaneously amplified and passed to an A/D converter with a desired time interval. The conversion time was 1 μs for one channel. By means of the previous calibration for temperature-resistance relationship, the average temperature of experimental minichannel ($T_a(t)$) was acquired as follows:

$$R_T(t) = R_0(1 + \alpha T_a(t) + \beta T_a(t)^2) \tag{4}$$

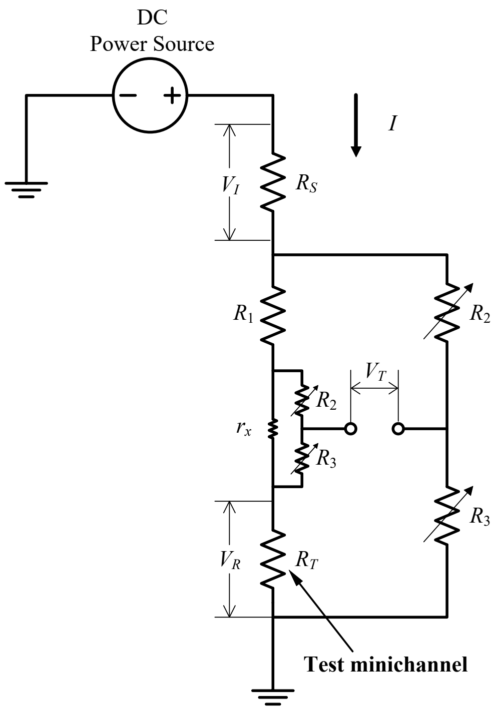

Fig. 2. The schematic diagram of the double-bridge circuit.

The heat flux on the inner surface of the experimental channel ($q(t)$) was calculated by an energy-balance equation:

$$q(t) = \frac{V}{A}\left(\dot{Q}(t) - \rho_h c_h \frac{dT_a(t)}{dt}\right) \tag{5}$$

where $\dot{Q}(t)$, V, A, c_h and ρ_h denote heat generation rate per unit volume, volume, inner surface area, specific heat and density of the experimental minichannel, respectively.

The instantaneous inner surface temperature of the experimental minichannel ($T_s(t)$) was calculated by solving the next unsteady heat conduction formula with the minichannel surface temperature being assumed as uniform:

$$\rho c \frac{\partial T}{\partial t} = \frac{1}{r}\frac{\partial}{\partial r}\left(r\lambda \frac{\partial T}{\partial r}\right) + \dot{Q}(t) \tag{6}$$

The boundary conditions are shown in the following equations with outer surface of the minichannel being assumed as adiabatic:

$$q(t) = -\lambda \frac{\partial T}{\partial r}\Big|_{r=r_i} \qquad \frac{\partial T}{\partial r}\Big|_{r=r_o} = 0$$

(7)

Furthermore, the heat generation rate increased slowly with a long elapsed time under a steady-state condition. Therefore, the $\dot{Q}(t)$ was approximated to $\dot{Q}$ as well as $q(t)$ being approximated to q for the steady state [25]. The solutions of the T_s were acquired by solving the next steady-state heat conduction equation associated with the boundary conditions:

$$\frac{d^2T}{dr^2} + \frac{1}{r}\frac{dT}{dr} + \frac{\dot{Q}}{\lambda} = 0 \tag{8}$$

$$q = -\lambda \frac{dT}{dr}\Big|_{r=r_i} \qquad \frac{dT}{dr}\Big|_{r=r_o} = 0$$

(9)

The average temperature (T_a) and temperature distribution ($T(r)$) of the experimental minichannel were given by:

$$T(r) = -\frac{\dot{Q}r^2}{4\lambda} + \frac{\dot{Q}r_o^2}{2\lambda}\ln r + C \tag{10}$$

$$T_a = \frac{1}{\pi(r_o^2 - r_i^2)}\int_{r_i}^{r_o} 2\pi r T(r)\,dr \tag{11}$$

where

$$C = T_a - \frac{q r_i}{4(r_o^2 - r_i^2)^2 \lambda} \times \left[4 r_o^2 \left\{ r_o^2 \left(\ln r_o - \frac{1}{2} \right) - r_i^2 \left(\ln r_i - \frac{1}{2} \right) \right\} - (r_o^4 - r_i^4) \right] \quad (12)$$

Then, the inner (T_s) and outer (T_{so}) surface temperature of the experimental minichannel were expressed as:

$$T_s = T(r_i) = T_a - \frac{q r_i}{4(r_o^2 - r_i^2)^2 \lambda} \times \left[4 r_o^2 \left\{ r_o^2 \left(\ln r_o - \frac{1}{2} \right) - r_i^2 \left(\ln r_i - \frac{1}{2} \right) \right\} - (r_o^4 - r_i^4) \right] - \frac{q r_i}{2(r_o^2 - r_i^2)\lambda} (r_i^2 - 2 r_o^2 \ln r_i) \quad (13)$$

$$T_{so} = T(r_o) = T_a - \frac{q r_i}{4(r_o^2 - r_i^2)^2 \lambda} \times \left[4 r_o^2 \left\{ r_o^2 \left(\ln r_o - \frac{1}{2} \right) - r_i^2 \left(\ln r_i - \frac{1}{2} \right) \right\} - (r_o^4 - r_i^4) \right] - \frac{q r_i r_o^2}{2(r_o^2 - r_i^2)\lambda} (1 - 2 \ln r_o) \quad (14)$$

The estimated maximum uncertainties of the $\dot{Q}$, q, and T_s were ±2%, ±2.4%, and ±1 K, respectively [22, 23].

The outlet temperature of helium gas (T_{out}) was obtained by the next energy-balance expression:

$$T_{out} = T_{in} + \frac{4 L_e q}{u c_{p,g} \rho_g d} \quad (15)$$

where T_{in}, u, $c_{p,g}$ and ρ_g are inlet temperature, average flow velocity, specific heat at constant pressure, and density of helium gas, respectively. In addition, the mean bulk temperature of helium gas (T_g) ($= (T_{in} + T_{out})/2$) was used as the reference temperature to evaluate all physical properties.

2.3. Experimental procedure and conditions

The whole loop was initially vacuumized by the vacuum pump and filled with helium gas to a desired pressure. Then, the helium gas was pumped to circulate in the loop by running the compressor. The helium gas before inlet of the experimental minichannel was heated to a designated temperature by using the pre-heaters. The heated gas departing from the test section was cooled in the cooler. By using the valves of the by-pass loops, the flow velocity was changed in order. After the temperature, pressure and flow velocity became stable, the heat generation rate of the experimental minichannel ($\dot{Q}$) was raised with an exponential function:

$$\dot{Q} = Q_0 \exp(t/\tau) \quad (16)$$

where Q_0, t, and τ represent initial heat generation rate, time, and e-folding time of the heat generation rate, respectively. In case of tube burn out, the current was cut off instantly when the tube temperature reached a pre-set value. When the τ was smaller than 0.1 s, the response time was fast. For the accuracy of experimental data, the experiment was conducted three times under the same experimental conditions as τ was smaller than 0.1 s. The heat transfer coefficient was the average value of these three tests. **Table 2** shows the experimental conditions in detail.

Table 2 The experimental conditions.

Inner diameters (d)	0.8, 1.8, 2.8 mm
Effective length (L_e)	90 mm
Thickness (δ)	0.1 mm
Inlet temperature (T_{in})	285-313 K
Inlet pressure (P_{in})	496-748 kPa
Flow velocity (u)	70-150 m/s
e-folding time (τ)	0.04-15 s

3. Experimental results and discussions

3.1. The time-varying $\dot{Q}$, q, ΔT and h

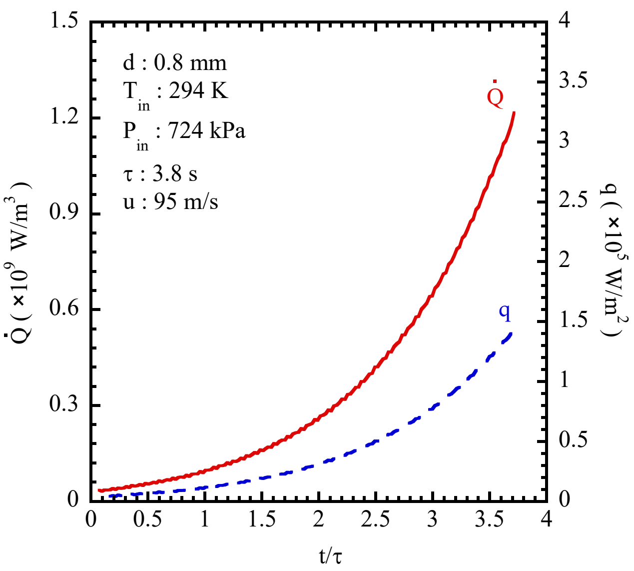

(a) d = 0.8 mm

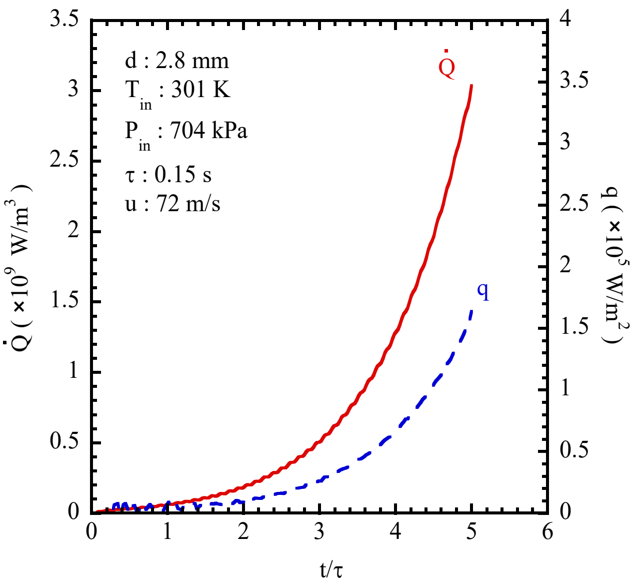

(b) d = 2.8 mm

Fig. 3. The time-varying $\dot{Q}$ and q.

Fig. 3 shows the representative experimental data of measured $\dot{Q}$ and q with time elapsed for the experimental minichannels with different inner diameters of 2.8 and 0.8 mm. The $\dot{Q}$ increases exponentially with time accompanying with an exponential increase in the q with time. This phenomenon was confirmed to be obtained for all experimental minichannels under different experimental conditions.

Fig. 4 shows the temperature difference between inner surface temperature of the experimental minichannel and the mean bulk temperature of helium gas (ΔT) ($= T_s - T_g$) as a function of the t/τ, and the instantaneous heat transfer coefficient (h) ($= q/\Delta T$) as a function of the t/τ under the same experimental conditions as **Fig. 3**. With an exponential increase in the ΔT caused by the exponentially increasing q, the initial high instantaneous h decreases to approach an asymptotic value. It can be understood that this asymptotic value is in the fully developed thermal condition. It is found that the asymptotic value is obtained under all experimental conditions and the region of the asymptotic value is dependent on different experimental conditions. For the 0.8 mm diameter minichannel under the τ of 3.8 s, the asymptotic value is obtained after the ΔT exceeds 15 K corresponding to the t/τ of 3. For the 2.8 mm diameter minichannel under the τ of 0.15 s, the asymptotic value is obtained after the ΔT exceeds 30 K corresponding to the t/τ of 4.3. The present research focuses on this asymptotic value, thus it is employed as a transient h for each τ under all experimental conditions.

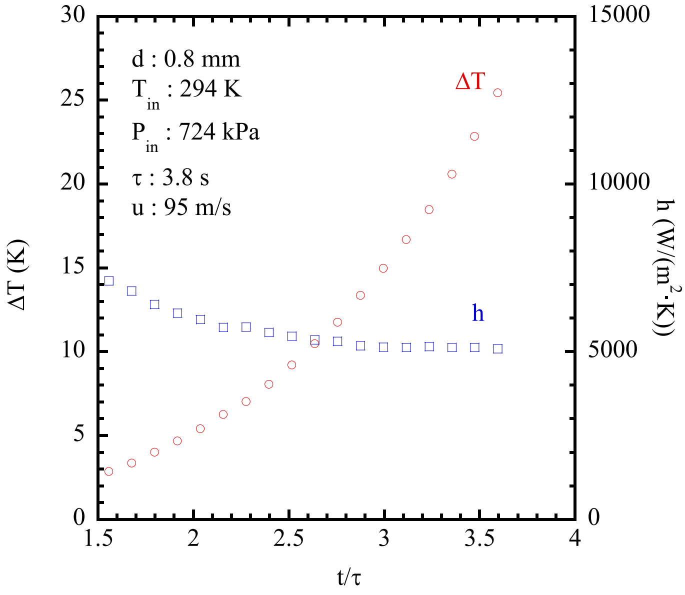

(a) d = 0.8 mm

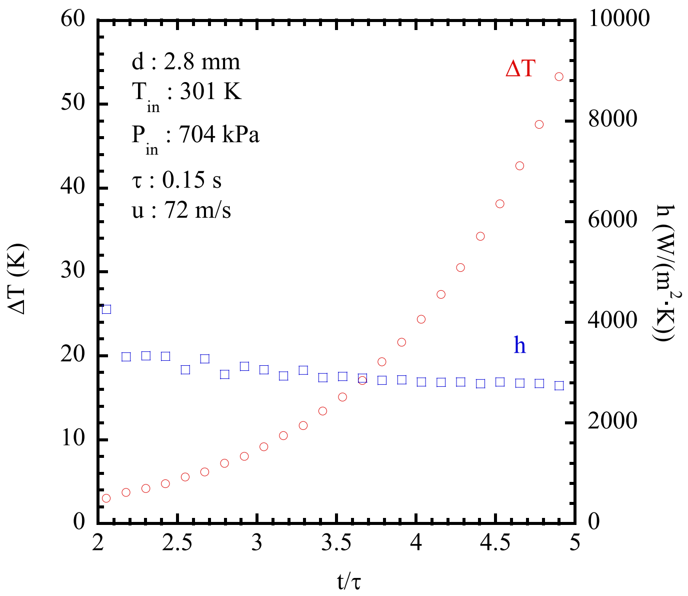

(b) d = 2.8 mm

Fig. 4. The time-varying ΔT and h.

3.2. Heat transfer process under transient and steady states

Fig. 5 (a) illustrates the variation of the h with τ varying from 0.08 to 15.3 s under the u in the range of 102-142 m/s for the 0.8 mm diameter minichannel. The h varies with τ ranging from 0.04 to 13.9 s under the u varying from 85 to 123 m/s for the 2.8

mm diameter minichannel, as illustrated in **Fig. 5 (b)**. Similar phenomena can be found in both 0.8 and 2.8 mm diameter minichannels. The h is affected by both the u and the τ. A higher h is acquired by a higher u for each τ. With an increase in the τ under the same u, the h decreases from a higher value as the τ is shorter than about 1.5 s and becomes an approximately constant value as the τ is longer than about 1.5 s.

For the τ over about 1.5 s, the effect of the τ on the h is not significant as a result of the thermal boundary layer being fully developed. It can be considered that the heat transfer in this region is in a quasi-steady state. More obvious influence of the u on the h is found in this region. It is indicated that the heat transfer by convection through the thermal boundary layer plays a dominant role in the quasi-steady condition. Further, the h for the τ over around 13 s can be defined as a steady-state h due to a relatively long response time.

For the τ shorter than about 1.5 s, an increase in the h with a decline of the τ is considered to be caused by a steeper temperature gradient and a thinner thermal boundary with decreasing τ. The temperature increase in the experimental minichannel is faster than the development of the thermal boundary layer [21]. It can be considered that the heat transfer in this region is under a transient condition. The influence of the u on the h becomes weak with decreasing τ in this region. The contribution of conductive heat transfer becomes larger with decreasing τ under the transient state.

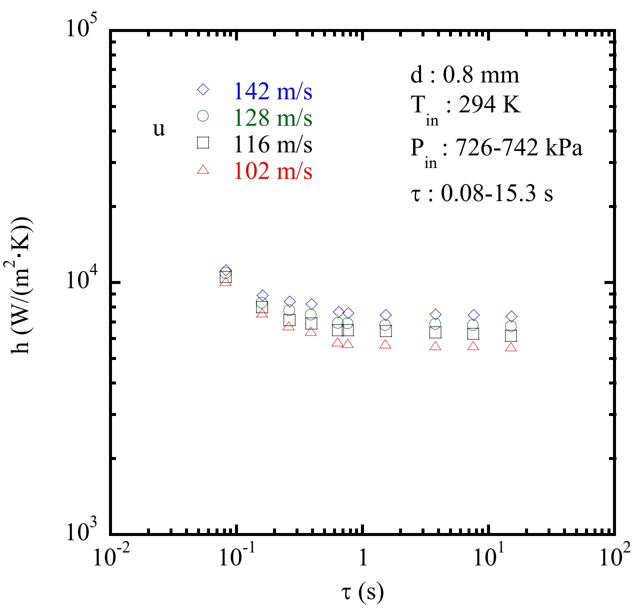

(a) $d = 0.8$ mm

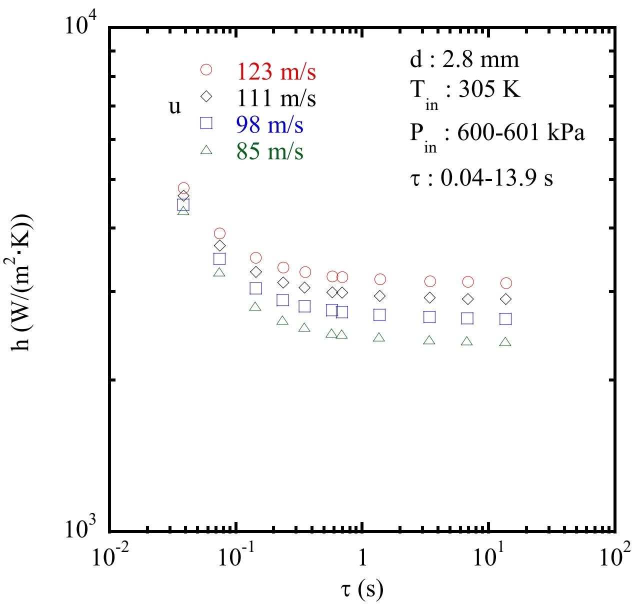

(b) d = 2.8 mm

Fig. 5. The variation of the h with τ under different u.

3.3. Comparison between the minichannels with different inner diameters

The h changed with τ for d = 0.8 mm is compared with that for d =1.8 mm at the same experimental conditions, as shown in **Fig. 6 (a)**. It is obvious that the heat transfer in the 0.8 mm diameter minichannel is significantly enhanced compared with the 1.8 mm under both transient and steady states. When the inner diameter of minichannel decreases from 1.8 to 0.8 mm, the h is raised by 66.1% at the τ of 15.0 s under the steady state and 73.1% at the τ of 0.26 s under the transient state.

Fig. 6 (b) shows the comparison of the h changed with τ between d = 1.8 mm and d = 2.8 mm. The h increases as the inner diameter of minichannel decreases from 2.8 to 1.8 mm, but the enhancement effect is not obvious under both transient and steady states. For the steady state, the h for d = 1.8 mm is 6.7% higher than that for d = 2.8 mm at the τ of 14.2 s. For the transient state, the increment of the h is 7.8% at the τ of 0.15 s.

The above result shows that the heat transfer enhancement for forced convective flow of helium gas in minichannels can be obtained by decreasing the minichannel inner diameters for both transient and steady states. It is supposed that the friction in the minichannel becomes stronger and the conductive sublayer near the inner surface of minichannel becomes thinner as the inner diameter of minichannel decreases [10].

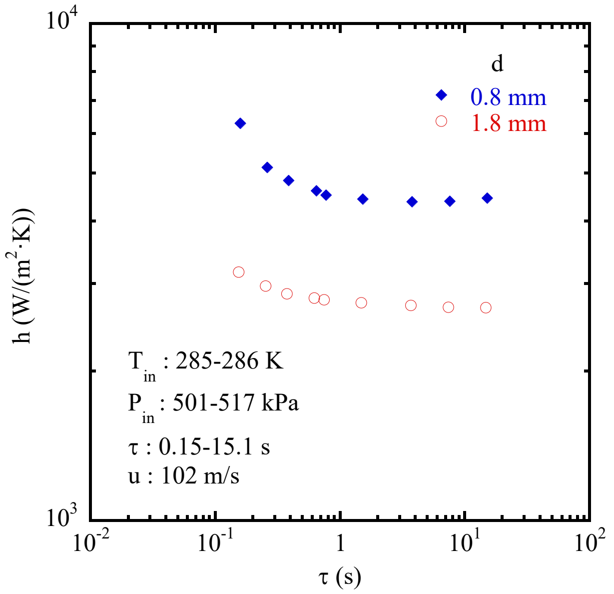

(a) d = 0.8 mm and d =1.8 mm

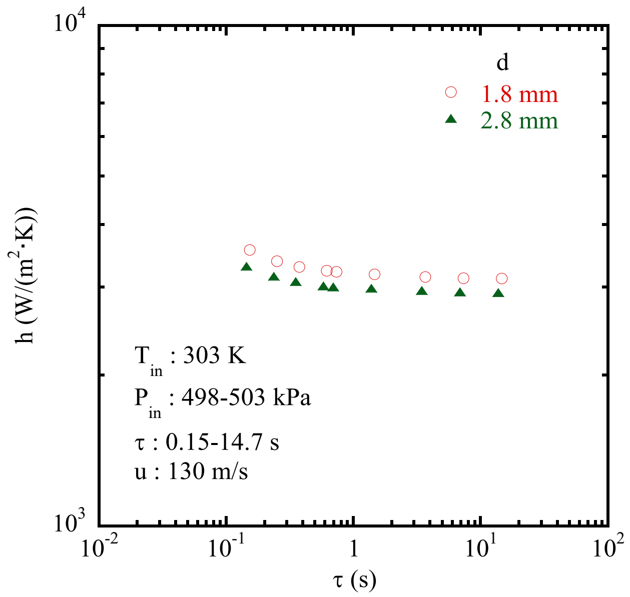

(b) d = 1.8 mm and d = 2.8 mm

Fig. 6. The comparison of the h between the experimental minichannels with different inner diameters under various τ.

3.4. Correlation for the steady-state heat transfer

The heat transfer correlations of steady-state experimental data for d = 0.8 mm and d = 2.8 mm are developed with reference to the correlation for d = 1.8 mm in the previous work [22]. As mentioned in the Section 3.2, the h for the τ over about 13 s is defined as the steady-state h (h_{st}). The steady-state Nusselt number (Nu_{st}) ($= h_{st}d/\lambda$), Renolds number (Re) ($= ud/\nu$), Prandtl number (Pr) ($= \nu/a$), and temperature correction factor $(T_s/T_g)^{-0.5}$ are introduced for the correlations. The correlation of steady-state heat transfer for d = 1.8 mm is used for comparison as shown in the following equation [22]:

$$Nu_{st} = 0.0333Re^{0.8}Pr^{0.4}(T_s/T_g)^{-0.5}$$

(d: 1.8 mm; Re: 5000-16000; deviation: ±10%) (17)

The steady-state heat transfer correlation for d = 0.8 mm is obtained from the experimental data of the present work as follows:

$$Nu_{st} = 0.0203Re^{0.9}Pr^{0.4}(T_s/T_g)^{-0.5}$$

(d: 0.8 mm; Re: 2400-5200; deviation: ±10%) (18)

Fig. 7 shows the experimental data of $Nu_{st}/Pr^{0.4}/(T_s/T_g)^{-0.5}$ versus Re for d = 2.8 mm and d = 0.8 mm and steady-state heat transfer correlations for d = 1.8 mm and d = 0.8 mm. As illustrated in this figure, the measured data for d = 2.8 mm ($8350 < Re < 15350$) agree well with Eq. (17) in the turbulent region. Further, the measured data for d = 2.8 mm lie in -10% deviation of Eq. (17). It is attributed to that the h for d = 2.8 mm is slightly lower than that for d = 1.8 mm under the steady state, as mentioned in the Section 3.3. However, it can be considered that there is no significant difference between the inner diameters of 2.8 and 1.8 mm for the steady-state heat transfer of helium gas flowing in minichannels.

On the other hand, the measured data for d = 0.8 mm are depicted well by Eq. (18) within a deviation of ±10%, as illustrated in **Fig. 7**. The measured data for d = 0.8 mm as Re surpasses 5000 are obviously higher than those predicted by Eq. (17) used for d = 1.8 mm. By comparing the measured data for d = 2.8 mm and d = 0.8 mm with the steady-state heat transfer correlation for d = 1.8 mm, it is reconfirmed that the steady-state heat transfer for helium gas flowing in minichannels is enhanced as the inner diameter decreases. Further, the exponent of Re for Eq. (18) is 0.9, which is higher than 0.8 for Eq. (17). It means that the effect of Re on Nu_{st} for d = 0.8 mm is stronger than that for d = 2.8 mm and d = 1.8 mm.

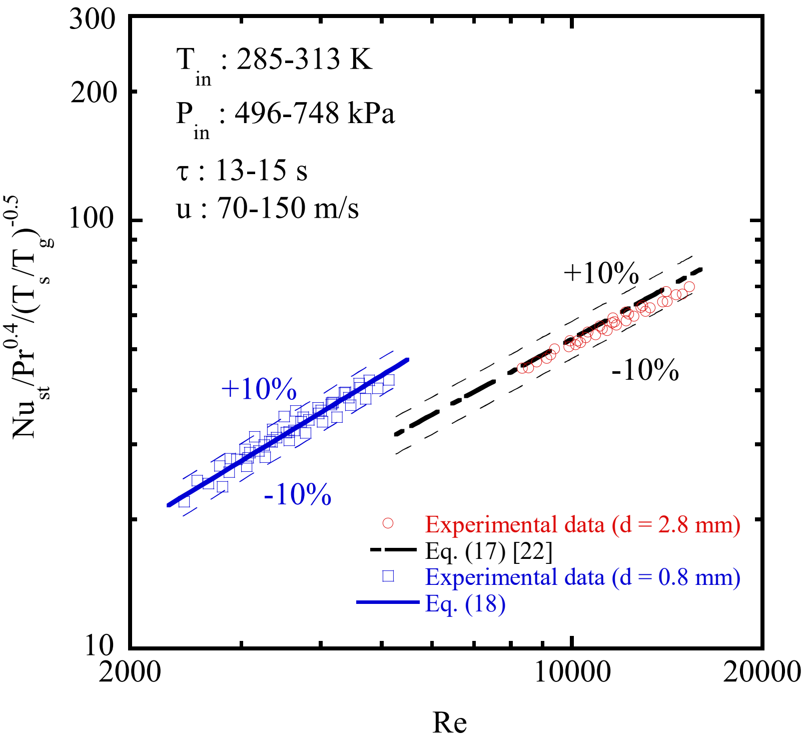

Fig. 7. The correlations for the steady-state heat transfer in the minichannels.

3.5. Correlation for the transient heat transfer

To understand transient heat transfer characteristics for forced convective flow of helium gas through the minichannels, a dimensionless parameter Fourier number (*Fo*) is used for analysis in the present research, as given by:

$$Fo = a\tau/d^2 \tag{19}$$

where *a* is the thermal diffusivity of test fluid. **Fig. 8** illustrates that *Nu* decreases from a higher value and approaches a constant value with an increase in the *Fo* for each *Re*. The variation trend of the relationship between *h* and *τ* for various *u* shown in **Fig. 5** is depicted well by the relationship between *Nu* and *Fo* for various *Re* at the same experimental conditions. For *d* = 0.8 mm, the quasi-steady-state and transient heat transfer can be distinguished at the *Fo* of around 87 (corresponding to the *τ* of about 1.5 s). And, the *Fo* of around 7 is corresponding to the *τ* of about 1.5 s for *d* = 2.8 mm. The *Nu* increases with a decrease in the *Fo* under the transient state. The *Nu* is not dependent on the *Fo* under the quasi-steady state.

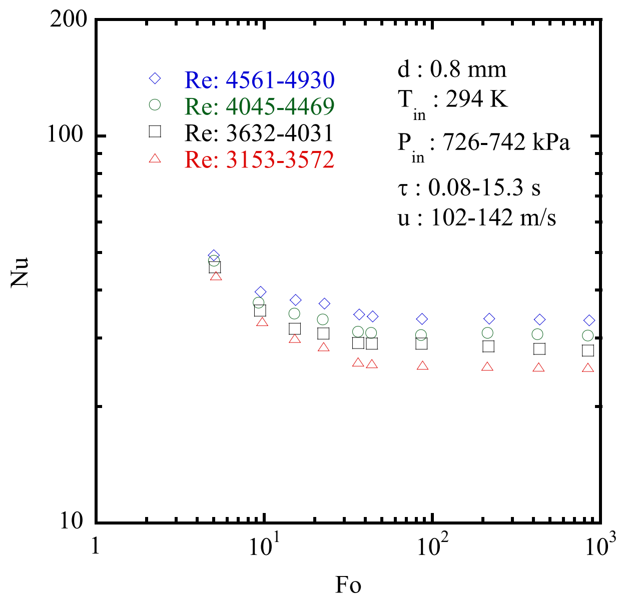

(a) $d = 0.8$ mm

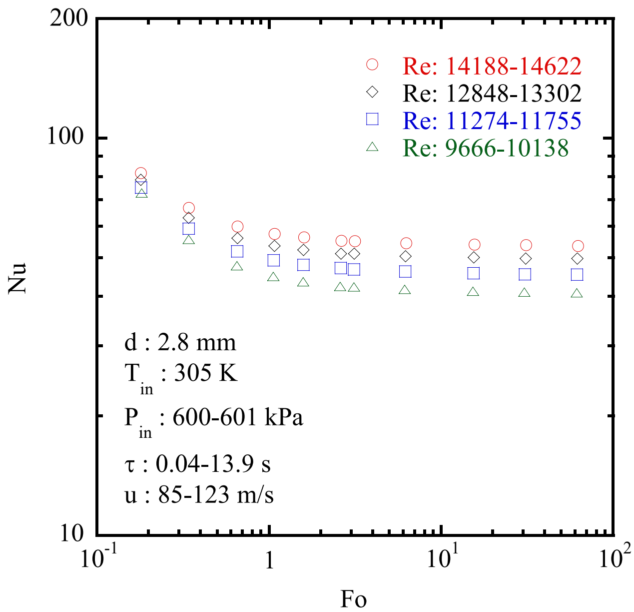

(b) $d = 2.8$ mm

Fig. 8. The relationship between *Nu* and *Fo* for various *Re*.

The relation of transient Nusselt number (Nu_{tr}) versus Nu_{st} for d = 1.8 mm was correlated by using *Fo* in the previous work [23]. The experimental data for d = 0.8 mm and d = 2.8 mm can be correlated by the same way. **Fig. 9** shows that the relationships between the ratio of Nu_{tr}/Nu_{st} and *Fo* for transient heat transfer of helium gas flowing in minichannels are correlated by the next equation:

$$Nu_{tr}/Nu_{st} = 1 + bFo^{-1.5} \quad (20)$$

where b is a constant dependent on the minichannel inner diameters. The values of b are 8.11, 0.362 [23], and 0.057 for d = 0.8 mm, d = 1.8 mm, and d = 2.8 mm, respectively. The deviations of the correlations for d = 2.8 mm and d = 0.8 mm are ±20% and ±15%, respectively. As Fo is larger than about 7 for d = 2.8 mm and about 87 for d = 0.8 mm, the approximately constant value of Nu_{tr}/Nu_{st} shows the quasi-steady-state heat transfer characteristics that are dominated by the convective heat transfer. Under the transient state as Fo is smaller than about 7 for d = 2.8 mm and about 87 for d = 0.8 mm, the ratios of Nu_{tr}/Nu_{st} start to increase with decreasing Fo. It is indicated that the contribution of conductive heat transfer start to increase with decreasing Fo under the transient state. Further, it can be considered that the boundary distinguishing between quasi-steady-state and transient heat transfer is obtained at a larger Fo with a decrease in the inner diameters of minichannels.

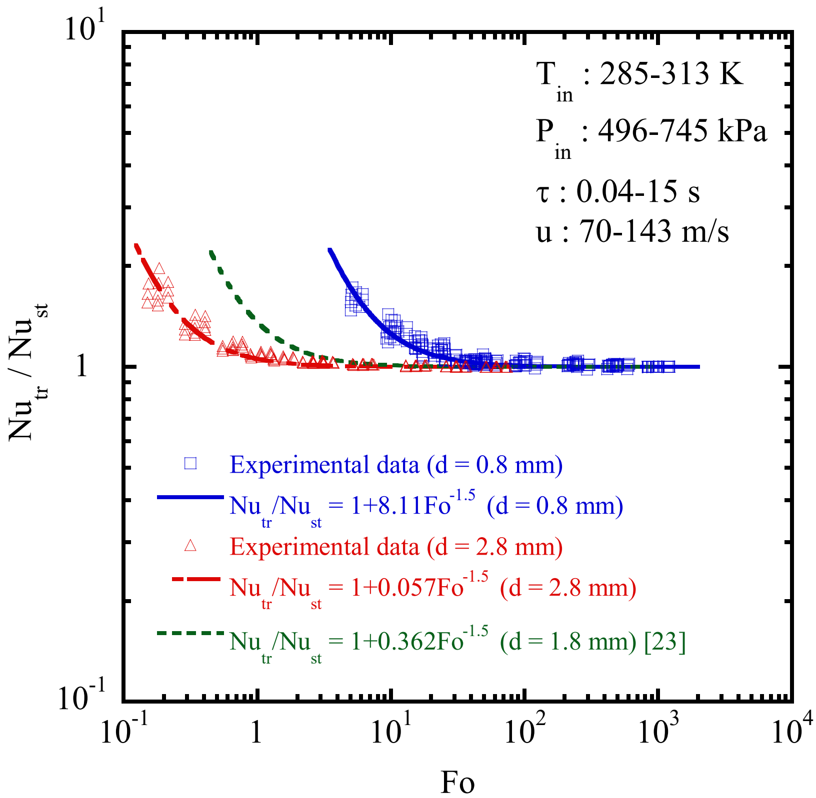

Fig. 9. The correlations for the transient heat transfer in the minichannels.

4. Conclusions

The heat transfer process under transient and steady states for helium gas flowing in minichannels with different inner diameters was experimentally investigated. The helium gas was utilized as test fluid and platinum minichannels were used as test tubes. The heat input increased exponentially with time. The results of the present work are shown as follows:

(1) The heat transfer coefficients under both transient and quasi-steady states increased with a decrease in the inner diameters of minichannels at the same experimental conditions. The difference on heat transfer coefficients between 1.8 mm and 2.8 mm diameter minichannels was not obvious but significant between 0.8 and 1.8 mm diameter minichannels.

(2) For the steady-state heat transfer, a correlation for the 0.8 mm diameter minichannel was acquired by the measured data of the present work. The measured data of the 2.8 mm diameter minichannel were within -10% deviation of the correlation for the 1.8 mm diameter minichannel. Compared to the 1.8 and 2.8 mm diameter minichannels, the Nusselt number was more dependent on Renolds number in the 0.8 mm diameter minichannel under the steady state.

(3) For the transient heat transfer, the correlations for the 0.8 and 2.8 mm diameter minichannels were developed by using Fourier number. As the inner diameters of minichannels decreased, the boundary distinguishing between quasi-steady-state and transient heat transfer was obtained at a larger Fourier number.

Acknowledgement

This work was funded by the Japan Society for the Promotion of Science (JSPS) (Grant-in Aid for Scientific Research (C), KAKENHI, No. 18K03979). The authors thank Mr. Yushi Honjo for his assistant to the experiment.

References

[1] K. Ehrlich, Materials research towards a fusion reactor, Fusion Engineering and Design 56-57 (2001) 71-82.

[2] T. Ihli, T.K. Basu, L.M. Giancarli, S. Konishi, S. Malang, et al., Review of blanket

designs for advanced fusion reactors, Fusion Engineering and Design 83 (2008) 912-919.

[3] H.L. Chen, M. Li, Z.L. Lv, G.M. Zhou, Q.W. Liu, et al., Conceptual design and analysis of the helium cooled solid breeder blanket for CFETR, Fusion Engineering and Design 96-97 (2015) 89-94.

[4] S.G. Kandlikar, Fundamental issues related to flow boiling in minichannels and microchannels, Experimental Thermal and Fluid Science 26 (2002) 389-407.

[5] T.S. Ravigururajan, M.K. Drost, Single-phase flow thermal performance characteristics of a parallel microchannel heat exchanger, Journal of Enhanced Heat Transfer 6 (5) (1999) 383-393.

[6] T.M. Adams, S.I. Abdel-Khalik, S.M. Jeter, Z.H. Qureshi, An experimental investigation of single-phase forced convection in microchannels, International Journal of Heat and Mass Transfer 41 (6-7) (1998) 851-857.

[7] P.S. Lee, S.V. Garimella, D. Liu, Investigation of heat transfer in rectangular microchannels, International Journal of Heat and Mass Transfer 48 (2005) 1688-1704.

[8] F.A. Hernández, F. Arbeiter, L.V. Boccaccini, E. Bubelis, V.P. Chakin, et al., Overview of the HCPB research activities in EUROfusion, IEEE Transactions on Plasma Science 46 (6) (2018) 2247-2261.

[9] A. Bucci, G.P. Celata, M. Cumo, E. Serra, G. Zummo, Water single-phase fluid flow and heat transfer in capillary tubes, in: Proceedings of the ASME 2003 1st International Conference on Microchannels and Minichannels, Rochester, New York, USA, 2003, pp. 319-326.

[10] Y.T. Li, Y.L. Ji, K. Fukuda, Q.S. Liu, Study on forced convective heat transfer of FC-72 in vertical small tubes, Journal of Thermal Science and Engineering Applications 12 (6) (2020) 061004.

[11] P. Naphon, O. Khonseur, Study on the convective heat transfer and pressure drop in the micro-channel heat sink, International Communications in Heat and Mass Transfer 36 (2009) 39-44.

[12] C.J. Ho, W.C. Chen, An experimental study on thermal performance of Al_2O_3/water nanofluid in a minichannel heat sink, Applied Thermal Engineering 50 (2013) 516-522.

[13] T. Dixit, I. Ghosh, Low Reynolds number thermo-hydraulic characterization of offset and diamond minichannel metal heat sinks, Experimental Thermal and Fluid

Science 51 (2013) 227-238.

[14] D.L. Chen, R. Granetz, B. Shen, F. Yang, J.P. Qian, et al., Characterization of plasma current quench during disruption in EAST tokamak, Chinese Physics B 24 (2) (2015) 025205.

[15] A. Cardella, H. Gorenflo, A. Lodato, K. Ioki, R. Raffray, Effects of plasma disruption events on ITER first wall materials, Journal of Nuclear Materials 283-287 (2000) 1105-1110.

[16] P.H. Abbrecht, S.W. Churchill, The thermal entrance region in fully developed turbulent flow, AIChE Journal 6 (2) (1960) 268-273.

[17] M. Soliman, H. A. Johnson, Transient heat transfer for forced convection flow over a flat plate of appreciable thermal capacity and containing an exponential time-dependent heat source, International Journal of Heat and Mass Transfer 11 (1) (1968) 27-38.

[18] Y.K. Prajapati, M. Pathak, M.K. Khan, Transient heat transfer characteristics of segmented finned microchannels, Experimental Thermal and Fluid Science 79 (2016) 134-142.

[19] Q.S. Liu, L. Wang, A. Mitsuishi, M. Shibahara, K. Fukuda, Transient heat transfer for helium gas flowing over a horizontal cylinder in a narrow channel, Experimental Heat Transfer, 30 (4) (2017) 341-354.

[20] Q.S. Liu, Z. Zhao, K. Fukuda, Transient heat transfer for forced flow of helium gas along a horizontal plate with different widths, International Journal of Heat and Mass Transfer 75 (2014) 433-441.

[21] Q.S. Liu, Z. Zhao, K. Fukuda, Experimental study on transient heat transfer enhancement from a twisted plate in convection flow of helium gas, International Journal of Heat and Mass Transfer 90 (2015) 1160-1169.

[22] F. Xu, Q.S. Liu, M. Shibahara, Experimental study on forced convection heat transfer of helium gas through a minichannel, International Journal of Heat and Mass Transfer 171 (2021) 121117.

[23] F. Xu, Q.S. Liu, M. Shibahara, Transient forced convective heat transfer of helium gas in a narrow tube heated by exponential time-varying heat source, Experimental Heat Transfer (published online) (2021) 1-20.

[24] Y.A. Cengel, J.M. Cimbala, R.H. Turner, Fundamentals of Thermal-Fluid Sciences, fourth ed., McGraw-Hill, New York, 2012, pp. 541-543.

[25] M. Shibahara, K. Fukuda, Q.S. Liu, K. Hata, Steady and transient critical heat flux

for subcooled water in a mini channel, International Journal of Heat and Mass Transfer 104 (2017) 267-275.